Academia Journal of Biotechnology 6(1): 001-011, January 2018
DOI: 10.15413/ajb.2018.0101
ISSN 2315-7747

Academia Publishing

Research Paper

Using a novel *Mucorindicus* CBS 226.29 ET for Biosynthesis of gold nanoparticles and applying them in nanoremediation of azo dyes

Alshehri A.N.Z.

Department of Biology, University College in Al-Jummum, Umm Al-Qura University, Makkah, 21955, Saudi Arabia. E-mail: anshehri@uqu.edu.sa. Tel: 00966563708094.

Accepted 5th February, 2018

ABSTRACT

Synthesis of nanoparticles by microorganisms may offer an environmentally friendly and affordable alternative to traditional physical and chemical methods. The microbial synthesis of nanoparticles is an approach based on green chemistry which mutually connects microbial biotechnology and nanotechnology. Fungus of *Mucorindicus* CBS 226.29 ET, in this work was used to synthesize gold nanoparticles (AuNPs). A surface level plasmon resonance peak was observed at 500 nm by UV-bis spectra of AuNPs. Images of AuNP through transmission electron microscope exhibited various shapes and dispersibility characteristics. The synthesis of AuNPs were optimum at the conditions 1.5 mM/L of HAuCl4, 0.6 g biomass and pH range 7 to 11. The decolorization of different azo dyes was catalyzed efficiently with the bio-AuNPs, and a new microbial resource candidate was thus demonstrated for these AuNPs through green synthesis, along with a potential bio-AuNP application for decolorization of azo dyes.

Keywords: *Mucorindicus*, biosynthesis, gold nanoparticles, decolorization, azo dyes.

INTRODUCTION

Superior characteristics of nanomaterials relative to bulk materials gave them a potential for application in every aspect of our lives (Kuang et al., 2013). The high oxidation resistance, stability and biocompatibility of gold nanoparticles (AuNPs) made them particularly more attractive than all other nanomaterials (Shukla et al., 2005; Bhumkar et al., 2007; Gong and Mullins, 2009). Although many traditional physical and chemical methods are available for the synthesis of AuNPs, their stability and concern over using toxic chemicals during production of AuNPs is considered problematic (Narayanan and Sakthivel, 2010; Das et al., 2010), hence, an urgent need exists for developing an eco-friendly process for synthesizing AuNPs. Compared to chemical and physical methods, biological methods for the synthesis of AuNPs is more reliable and ecofriendly (Zhang et al., 2011). Several micro-organisms can synthesize AuNPs, including bacteria, fungi and yeast (Zhang et al., 2011; Shedbalkar et al., 2014; Kitching et al., 2015).

Fungi offer great advantages for synthesizing AuNPs and are therefore considered to be most suitable for high nanoparticles production (Du et al., 2011; Girard et al., 2013). In particular, fungi secrete proteins and secondary metabolites in large quantities and extracellularly, which can then be separated easily without recourse to process of downstream (Mishra et al., 2014). Nevertheless, AuNP synthesis has only been investigated for fewer than 30 fungal species (Kitching et al., 2015). More fungi isolates need to be discovered for the biosynthesis of AuNPs and to overcome the major challenges related to shape, size and disparity. These three aforementioned major challenges have been shown in some reports to be affected by biomass and substrate concentrations and pH value (Gericke and Pinches, 2006; Pimprikar et al., 2009; Mishra et al., 2011).

The control of the size factor in AuNPs biosynthesis is very important given that particle size affects the nanomaterial properties directly. With respect to dyes, the largest chemical class is azo dyes which exhibit great

variety in structure and color (Tony et al., 2009), thus, serious and huge damage could occur in the environment by disposing effluents containing azo dyes. In particular, since dyes reflect and absorb sunlight due to their color content, wastewater can become contaminated which can thereby disrupt photosynthesis and affect aquatic organisms growth (Champagne and Ramsay, 2010). Some solutions for treating azo dye pollutants using green methods have been reported. For instance, some micro-organisms have been reported to be capable of treating azo dye pollutants efficiently such as *Pseudomonas, Shewanella* and *Bacillus* (Xu et al., 2007; Chen et al., 2011; Fang et al., 2015). The degradation of pollutants could be improved efficiently by using AuNPs in process of nanoremediation (Kumari and Philip, 2015). Reports on degradation of dyes by biogenic AuNPs are very rare.

In this work, the fungus *M. indicus* CBS 226.29 ET was used to synthesize AuNPs as eco-friendly method, and an UV-Vis spectrophotometer and Transmission Electron Microscopy (TEM) were used to determine the AuNPs characteristics. The optimum conditions of different parameters for biosynthesis of AuNPs were ascertained, and various azo dyes underwent decolorization to evaluate catalytic characteristics of the bio-AuNPs being prepared.

MATERIALS AND METHODS

Chemicals and medium

The chemicals used in this study were obtained from SIGMA ALDRICH Chemicals, USA. The selection and cultivation medium was a modified form of Martin Broth (MMB) at pH 7 consisting of (g/L): 1.0 $(NH_4)_2SO_4$, 1.0 KH_2PO_4, 0.5 $MgSO_4 \cdot 7H_2O$ and 1.0 glucose. The solid medium contained 2.0% (w/v) agar in MMB, and for isolating fungi strain 50 mg/L of each terramycin and tetracycline were added as selective pressure. Autoclaving of the media at a temperature of 115°C was done for 15 min prior to use.

Isolation and identification of fungus

Soil samples contaminated with heavy metals were collected from an industrial area in Jeddah-Saudi Arabia. The samples were then diluted serially prior to spreading onto MMB agar plates. Following a 4 day period of incubation at 30°C, selected colonies were transferred into 25 ml MMB medium and cultivated for a further period of 3 days at 30°C and at shaking of 150 r/min. A line of Lacto Phenol Cotton Blue (LPCB) was then smeared on a slide and examined under a confocal microscope. A sample of the fungal strain was picked up using adhesive tape and placed onto the LPCB for further examination by a confocal microscope (Leica, Wasteland, Germany). Subsequently, closer examination of the fungal strain was undertaken utilizing Scanning Electron Microscopy (SEM, JSM- 5410LV, JEOL Ltd., Japan) as described by Kim (2008).

Following a one month period of screening and enrichment, a single colony of *M. indicus* was selected to undergo further characterization and identification through 26S rRNA gene sequence analysis. Amplification of the 26S rRNA gene from DNA of the isolated fungus was achieved by Polymerase Chain Reaction (PCR), and sequencing of the PCR product was done by Center of Excellence in Genomic medicine Research-KAU (Saudi Arabia). The sequence was compared with those on record at GenBank using the BLAST program and related sequences were aligned by using Clustal X (1.8) for constructing a phylogenetic tree by the Neighbor -joining method using MEGA (version 5.1) with 1000 bootstrap replicates (Qu et al., 2010).

Synthesis of AuNPs

Fungus *M. indicus* CBS 226.29 ET was cultivated over a 2-day period in 100 ml MMB medium at 30°C and shaking at 150 r/min. Following incubation, the biomass of *M. indicus* CBS 226.29 ET was prepared by filtration and washing using sterile distilled water thrice. An appropriate wet biomass concentration was re-suspended in distilled water prior to further incubation over a period of 40 h at 30°C with 1.0 mM/L $HAuCl_4$, and a control experiment was also carried out without using any biomass. The following procedure was applied to investigate influences of concentrations of $HAuCl_4$ and biomass, as well as, pH values on synthesis of AuNPs: (1) Addition of $HAuCl_4$ in a range of concentrations (0.1, 0.5, 1.0, 1.5, 2.0, 5.0 mM/L) to the 0.1 g biomass solutions with a final volume of 4 ml; (2) Suspension of biomass with a range of mass (0.1, 0.2, 0.3, 0.4, 0.5, 0.6 g) in sterile distilled water (4 ml) were incubated with 2.0 mM/L of $HAuCl_4$; (3) Adjustment of the reaction solution to pH (3, 5, 7, 9, 11) was done by HCl and NaOH. These aforementioned experiments were carried out for 40 h at a temperature of 30°C.

Characterization of AuNPs

Examination of AuNPs formation was done by visually observing color changes of the suspensions before monitoring with a UV-Vis spectrophotometer (Metash UV-9000, China) to record spectra ranging between 400 and 800 nm at 1 nm resolution. AuNP morphology was then characterized using a Transmission Electron Microscope (TEM) (Tecnai G2 Spirit-FEI, Netherlands) with 120 kV accelerating voltage. Samples of 15 µl were dropped for the TEM analysis onto a carbon coated copper grid, which was then dried at room temperature prior to the analysis.

Decolorization of azo dyes by bio-AuNPs

The *M. indicus* CBS 226.29 ET and AuNPs were subjected to

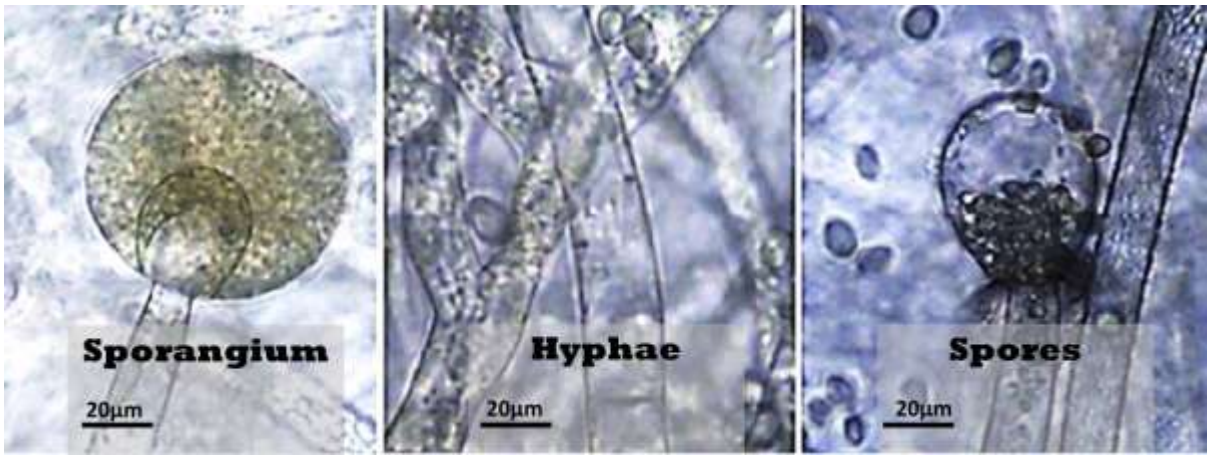

Figure 1: Images of the isolated fungal strain under confocal microscope show the morphological features.

ultrasonication process (Ultrasonic Processor CPX 750, USA) to produce bio-AuNPs for decolorization of azo dyes. Acid, reactive and cationic azo dyes were used to demonstrate potential catalytic activity of the bio-AuNPs in decolorization of azo dyes. After addition of dyes to 50 mg/L of the bio-AuNP solution and incubation on the shaker at 30°C and 150 r/min, a control experiment was conducted using ultrasonicated *M. indicus* CBS 226.29 E cells under identical conditions instead of bio-AuNPs for decolorization of 50 mg/L of Acid Brilliant Scarlet GR. The influence of initial concentration of Acid Brilliant Scarlet GR (25, 50, 100, 200 mg/L) on decolorization process was examined.

Analytical methods

The absorption wavelength of azo dyes (λ_{max}) was scanned as characteristic to monitor the decolorization process using a UV–Vis spectrophotometer following centrifugation (10,000 g) for 5 min at varying time intervals. The following equation was used to calculate the decolorization proportion:

$$\text{Decolorization (\%)} = (A_0 - A_1)/=A_0 \times 100 \quad (1)$$

Where A_0 and A_1 represent the dye's initial and final absorbance respectively.

High Performance Liquid Chromatography-Mass Spectrometry (HPLC-MS) was used to detect the intermediate products, which resulted from reduction of Acid Brilliant Scarlet GR by bio-AuNPs, as earlier described (Tan et al., 2013).

RESULTS AND DISCUSSION

Isolation and identification of *M. indicus*

A fungal strain identified as *M. indicus*, was isolated from a sample of contaminated soil with heavy metals taken from Jeddah-Saudi Arabia. Initial screening of the fungal specimen on its third day of growth prepared using adhesive tape revealed highly grown hyphae, sporangium-like structures and spores under confocal microscope (Figure 1). For finer details, the fungal strain was examined by SEM. The hyphae, collumella, sporangium, sporangiospore and collarette of the strain were clearly observed (Figure 2). All of these notable features were attributed to the genus *Mucor*, and based on the morphological specifications, it was clear that the fungal strain would belong to the genus *Mucor*. Morphological specifications are usually sufficient to determine a strain's genus level, but rDNA sequencing is necessary for distinguishing micro-organisms at the level of species. Analysis of the 26S rRNA gene sequence showed evidence of 100% homology of the fungus to *M. indicus* (Genebank accession number CBS 226.29 ET); consequently, the identification of the fungus was *M. indicus* CBS 226.29 ET. The relationship between *M. indicus* CBS 226.29 ET and other strains was demonstrated in the phylogenic tree as depicted in Figure 3.

Biosynthesis of AuNPs

Biosynthesis of the AuNPs was done by incubating *M. indicus* CBS 226.29 ET with $HAuCl_4$. After 4 h of incubation, the reaction mixture changed from a pale yellowish color to violet (Figure 4). This indicated the formation of gold nanoparticles, and the color change was indicative of a coherent oscillation of surface nanoparticles of electron gas resulting in surface plasmon resonance (SPR) (Kitching et al., 2015). An absorption peak was observed at 500 nm by UV-vis spectrum of the reaction solution (Figure 5). This was indicative of AuNPs formation (Kalishwaralal et al., 2009).

The dispersion of synthesized AuNPs was characterized by a diversity of shapes, as shown by the TEM images. The

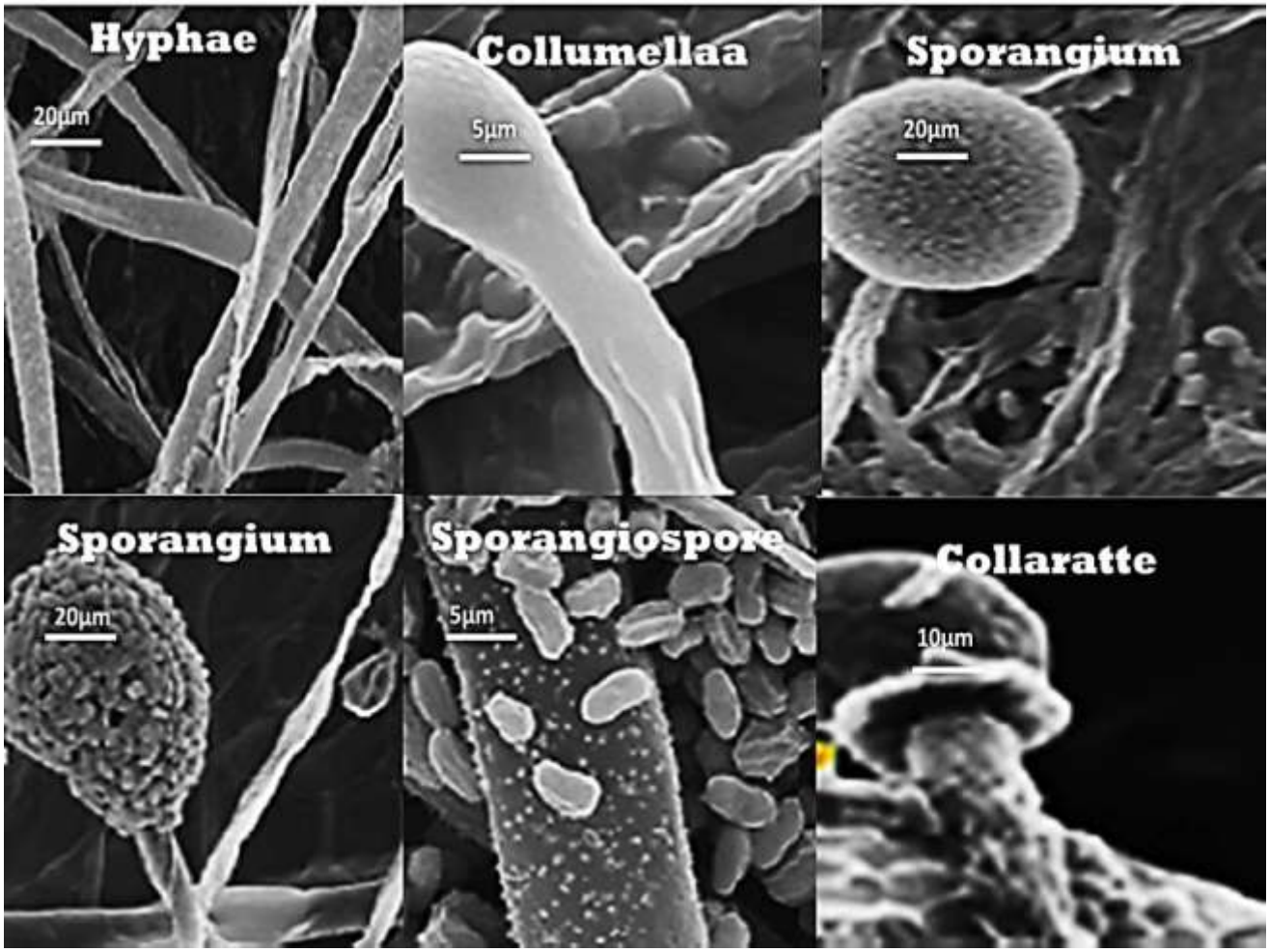

Figure 2: SEM images of the isolated fungal strain show the morphological features.

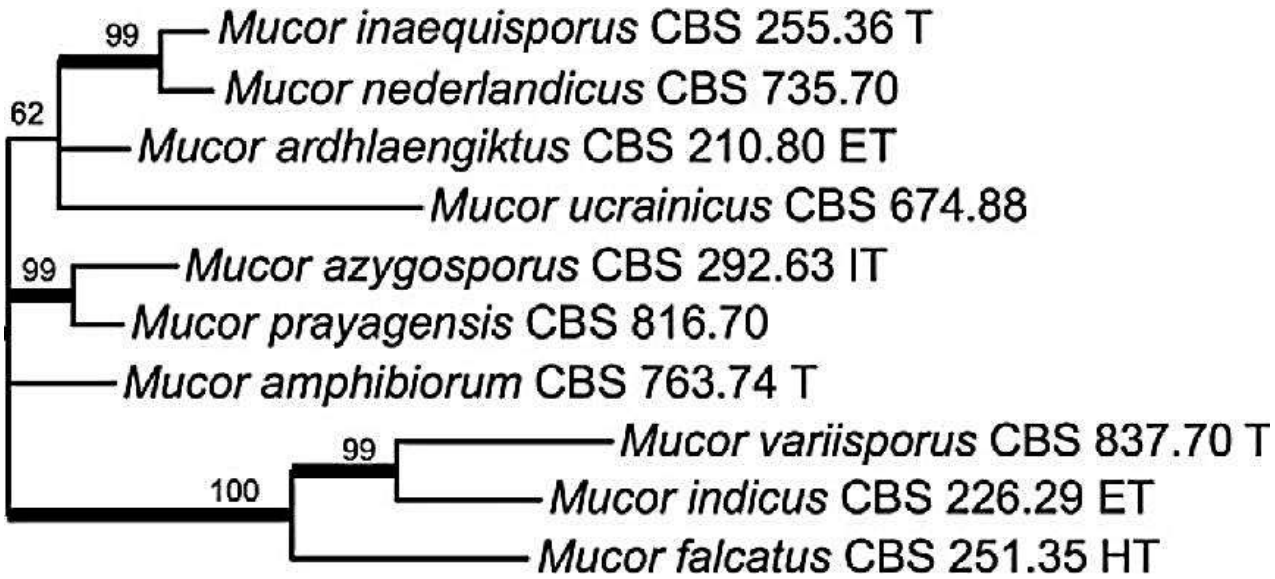

Figure 3: Phylogenetic tree of *M. indicus* CBS 226.29 ET and related species.

Figure 4: The pale yellowish reaction mixture A changed to violet color B, indicating the formation of gold nanoparticles.

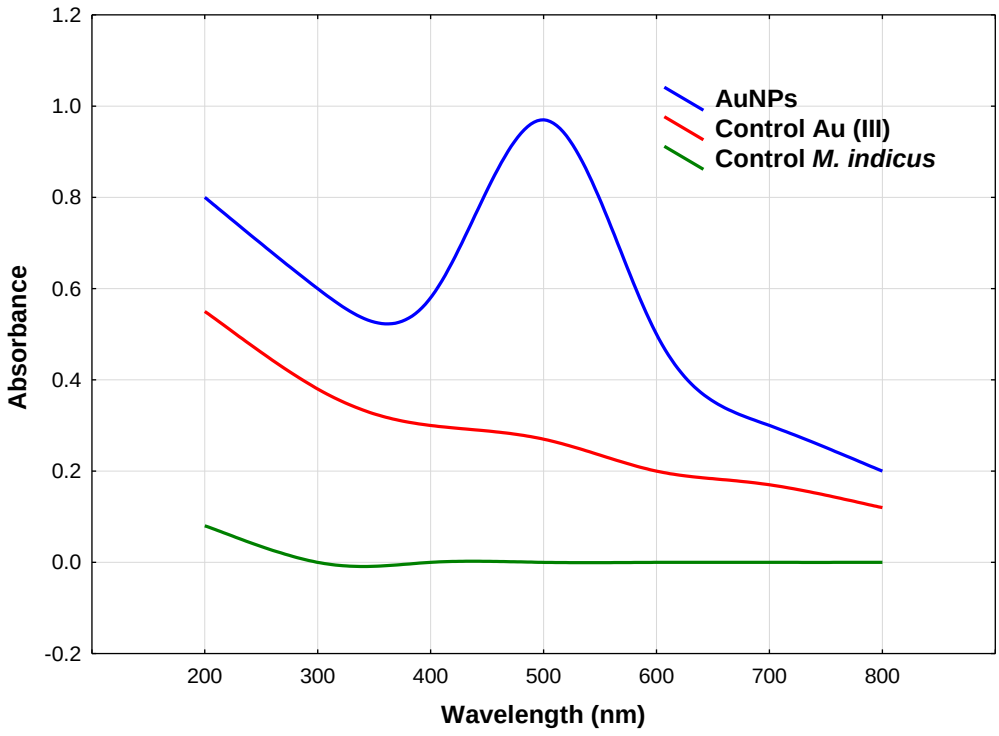

Figure 5: UV–vis spectra of the dispersed AuNPs synthesized by strain *M. indicus* CBS 226.29 ET after 40 h incubation, $HAuCl_4$ solution, and control strain *M. indicus* CBS 226.29 ET.

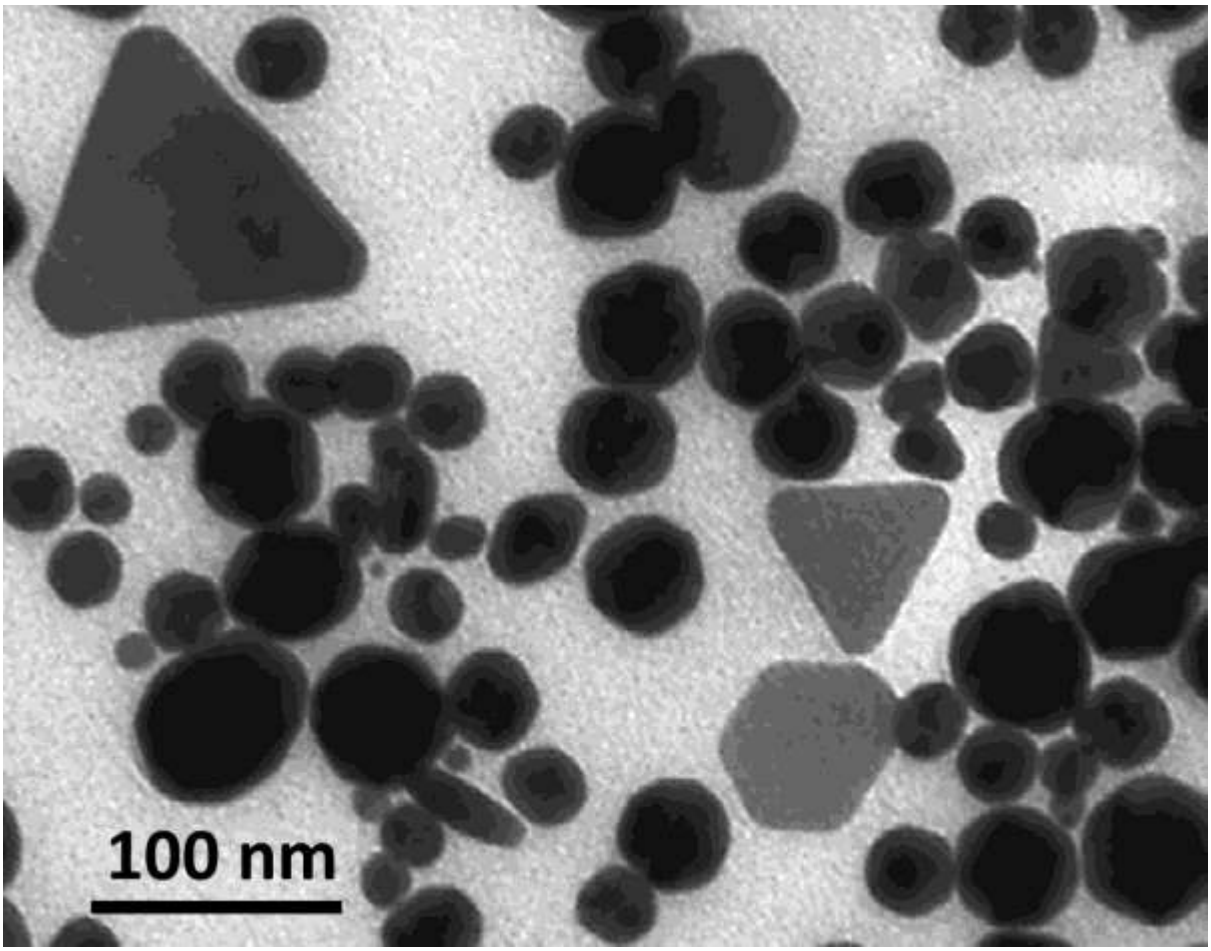

Figure 6: The TEM image of AuNPs synthesized by strain *M. indicus* CBS 226.29 ET.

predominant shape was the sphere, but triangles and hexagons were also observed, and with respect to size, spherical particles were found to be smaller relative to the triangles and polygons (Figure 6). As a genus, the fungal strain *M. indicus* is known to be capable of secreting a range of extracellular enzymes and metabolites in varying amounts. This advantage makes it a highly suitable candidate for producing metal nanoparticles on an industrial scale (Vahabi et al., 2011; Morin-sardin et al., 2017). The results also confirmed that *M. indicus* have exemplary ability in the biosynthesis of AuNPs, which makes them further suitable for AuNPs biosynthesis as a potential microbial resource.

Effect of $HAuCl_4$ concentrations

Figure 7 depicts the effects of the $HAuCl_4$ concentrations (0.5, 1.5, and 2.0 mM/L) on the synthesis of AuNPs. A violet or pink color was observed for those suspensions treated with $HAuCl_4$ for 40 h. Absorption peaks were recorded at 500 nm confirming AuNPs formation (Song et al., 2009), and when the concentration was 1.5 mM/L, a strong Surface Plasmon Resonance (SPR) band was observed at 500 nm. Thus, the optimal concentration of $HAuCl_4$ was 1.5 mM/L for AuNPs biosynthesis. Increasing the $HAuCl_4$ concentration to 5.0 mM/L resulted in the synthesis of gold particles at large sizes achieved by attaching on the tube wall. Large particle formation was likely to be due to a lack of biomolecules necessary for capping the synthesized nanoparticles and their efficient stabilization (Kumari and Philip, 2015). The use of *Verticillium luteoalbum* for AuNPs synthesis resulted in a similar observation. A concentration of $HAuCl_4$ below 500 mg/L resulted in a particle size of around 20 nm, whereas a concentration above 500 mg/L resulted in a distribution of the particle size from 50 nm to several hundred nanometers. Furthermore, the cells exhibited massive particle aggregates (Gericke and Pinches, 2006).

Effect of biomass concentrations

Figure 8 illustrates the effects of biomass concentrations on the synthesis of AuNPs. The color of all the reactive solutions changed to purple indicating synthesis of AuNPs

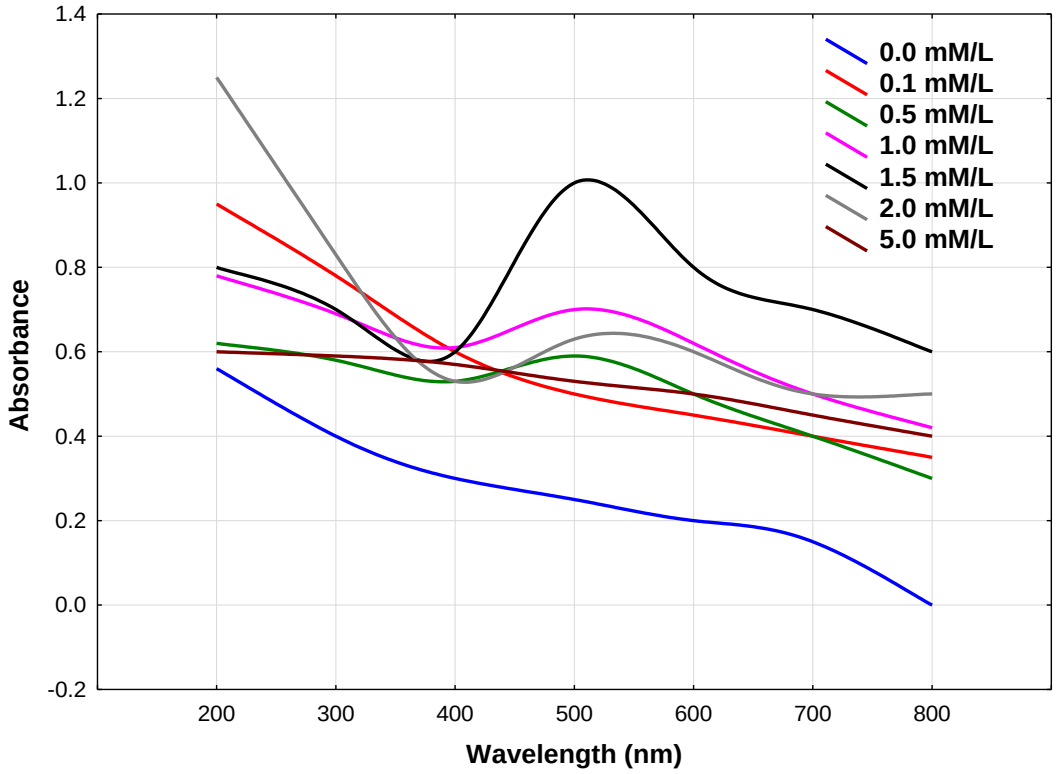

Figure 7: UV–Vis spectra of the dispersed AuNPs synthesized under different concentrations of $HAuCl_4$ (0.1, 0.5, 1.0, 1.5, 2.0, 5.0 mM) in reaction solutions.

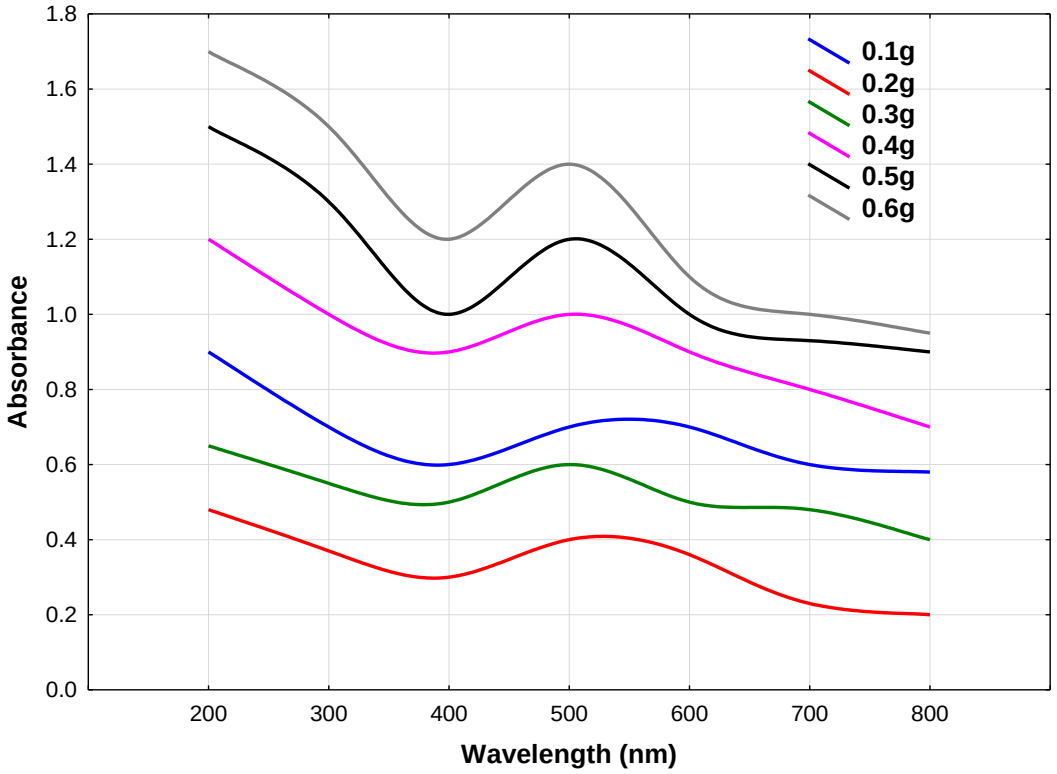

Figure 8: UV–Vis spectra of the dispersed AuNPs synthesized under different concentrations of strain *M. indicus* CBS 226.29 ET biomass (0.1, 0.2, 0.3, 0.4, 0.5, 0.6 g) in reaction solutions.

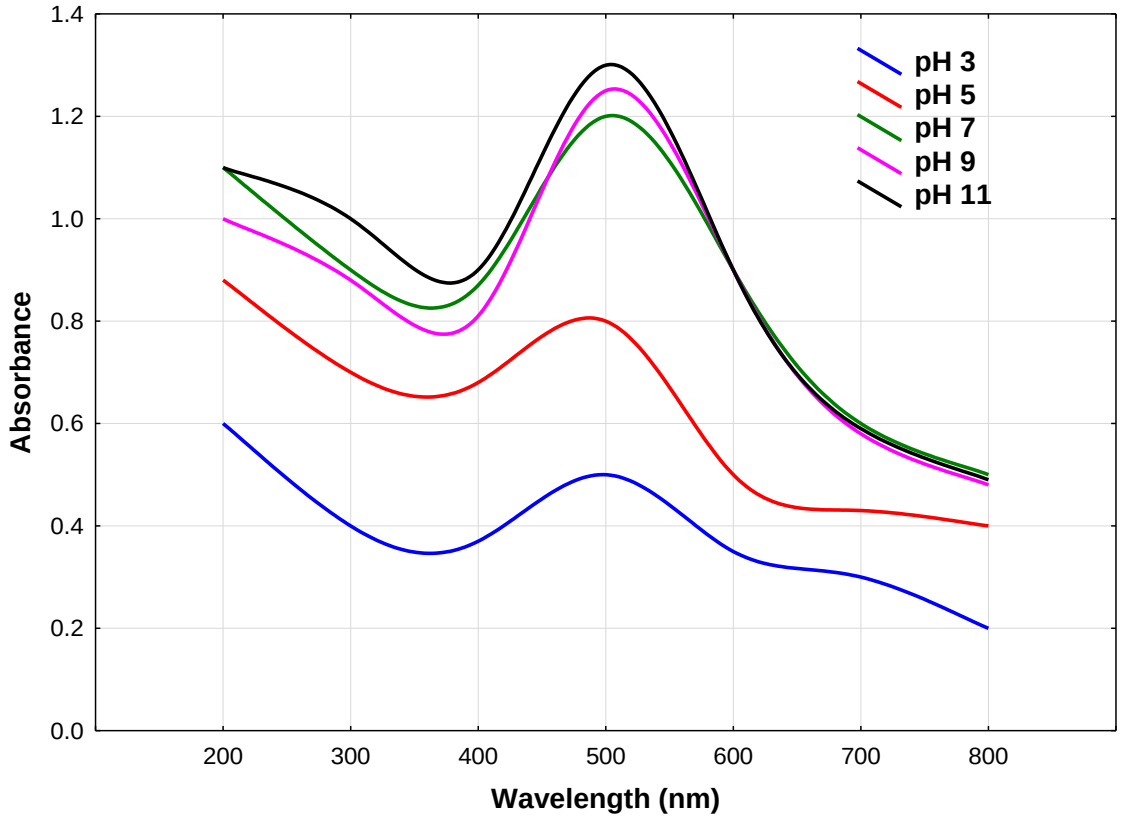

Figure 9: UV–Vis spectra of the dispersed AuNPs synthesized under different conditions of pH (3, 5, 7, 9, 11) in reaction solutions.

at varying biomass concentrations. When using 0.1 g of biomass, a broadening of the Surface Plasmon Resonance (SPR) absorbance of reaction solution was displayed at the maximum wavelength of 500 nm. This broadness may be attributed to large formations of AuNPs (triangle, hexagon and sphere) causing a transverse interaction of radiance (Kreibig and Genzel, 1985; Sujitha and Kannan, 2013). Notably, when the biomass concentration was increased to 0.6 g, a narrowing of the absorbance band was evident along with a blue shift. This may be explained as higher biomass concentrations providing more biomolecules thereby reducing gold ions and allowing for the synthesis of smaller sized particles and hence, the blue shift in absorption peak levels (Haiss et al., 2007).

Effect of pH

The influence of pH values on synthesis of AuNPs is illustrated in Figure 9. An improvement in the average of AuNP synthesis was spotted when increasing the pH value of solutions. In a condition of extreme alkalinity (pH 12), the color was observed to change within 2 h as compared to 4 h when in a condition of extreme acidity (pH 3). The SPR band was strongly and sharply defined when in the range pH 7 to 11, but relatively broader at pH 3. These sharpness and strength at pH 7 to 11, interpreted as a better performance at synthesis of AuNPs, may be explained as being due to a higher stability of capping proteins, which the *M. indicus* CBS 226.29 ET secreted under either alkaline or neutral conditions, whereas under acidic conditions, protonation of the carboxylic groups may occur (Bastús et al., 2011). Mishra et al. (2011) also observed this phenomenon, thereby, confirming the ability of the cell free extract of *Trichoderma viride* to synthesize AuNPs, which took place at pH 7 and 9, but not pH 5.

Application of bio-AuNPs for azo dye decolorization

Employing of bio-AuNPs in nanoremediation process as a decolorative to remove azo dyes was conducted. Figure 10 displays the decolorization of various azo dyes due to bio-AuNPs. This includes four acid azo dyes by rate 81 to 96% in 100 to 120 min, three reactive azo dyes by rate 45 to 70% in 100 to 180 min, and one cation azo dye by rate 39% in 180 min. The maximum efficiency in decolorization was for Acid Brilliant Scarlet GR at 94.7%. This was therefore selected as a model dye in further experimental investigation. Figure 11 displays different concentrations of Acid Brilliant Scarlet GR undergoing decolorization processes by the bio-AuNPs. The efficiency of Acid Brilliant

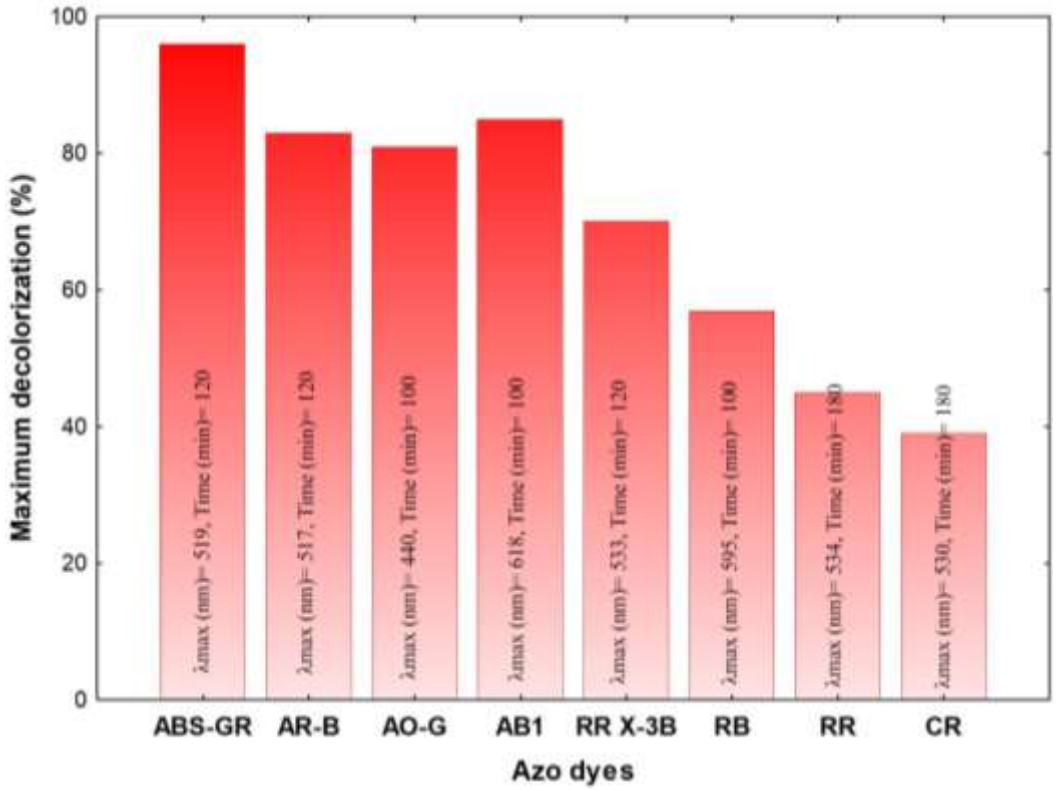

Figure 10: Decolorization of azo dyes (50 mg/L) by bio-AuNPs. Acid Brilliant Scarlet GR (ABS-GR), Acid Red B (AR-B), Acid Orange G (AO-G), Acid Black 1 (AB1), Reactive Red X-3B (RR X-3B), Reactive Black (RB), Reactive Red (RR), Cation Red (CR).

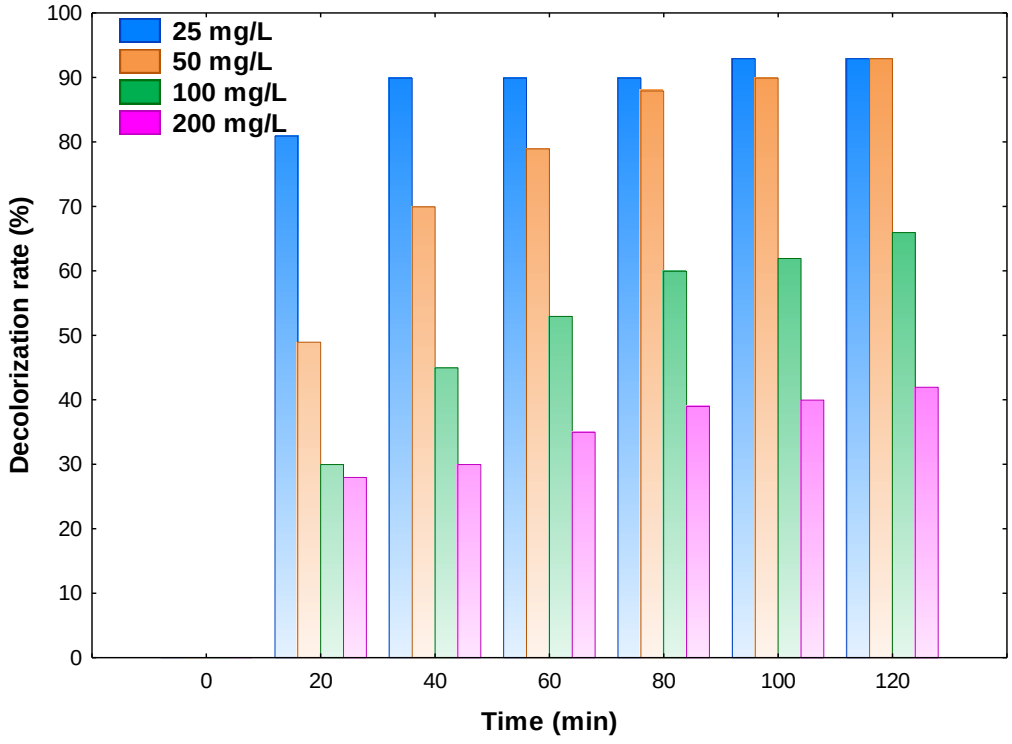

Figure 11: Effects of initial concentration (25, 50, 100, 200 mg/L) of Acid Brilliant Scarlet GR on decolorization.

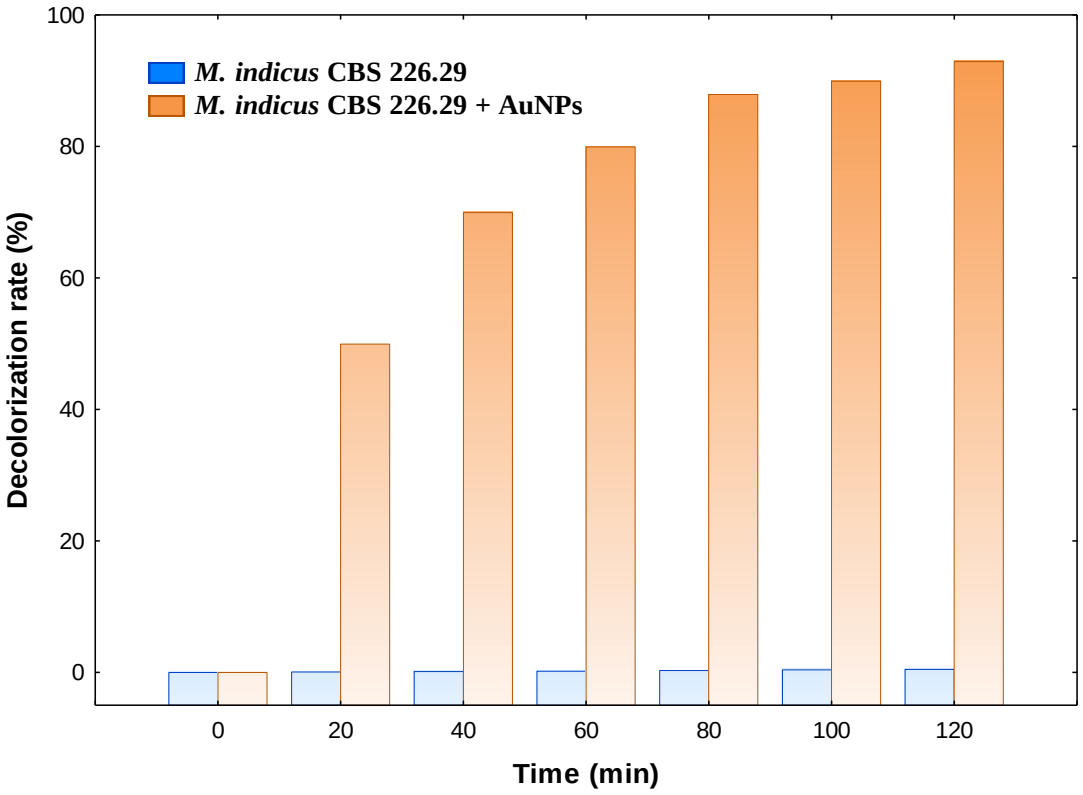

Figure 12: The decolorization rate of Acid Brilliant Scarlet GR (50 mg/L) by ultrasonicated*M. indicus* CBS 226.29 ET cells and bio-AuNPs (mixture of AuNPs and ultrasonicated*M. indicus* CBS 226.29 ET cells).

Scarlet GR in decolorization was found to be greater than 90% over 40 min for a dye concentration of 25 mg/L. When this concentration was increased to 50 mg/L, the high efficiency over 90% in 100 min was retained, but ultrasonicated *M. indicus* CBS 226.29 ET cells decolored only 4.8% of Acid Brilliant Scarlet GR (Figure 12). AuNPs may therefore enhance decolorization greatly with the use of high catalytic activities.

Analysis of Acid Brilliant Scarlet GR decolorization by-products by HPLC-MS revealed two candidates functioning as decolorization intermediates, namely 3, 7-Dihydroxyoctahydronaphthalene- 2, 6-dione (I) corresponding to a mass peak of 215.1658 ([M–H^+]) and naphthol (II) that was emphasized with m/z ion peak of 143.1078 ([M–H^+]). Previous reports have also detected the same as intermediates of Acid Brilliant Scarlet GR degradation (Gomi et al., 2011; Tan et al., 2013). In early study, Dos et al. (2007) indicated that the first step of azo dye degradation was reductive cleavage of azo groups (–N=N–), however, this study did not detect 1-aminonaphthylene-2- hydroxy-3, 6-disulfonic acid (III) as corresponding amines of Acid Brilliant Scarlet GR to which it was initially transformed. Oxidation of the intermediate (III) was likely to have been under aerobic conditions to the compound (I) (Tan et al., 2013). The generation of intermediate (II) from product (I) was likely a result of the removal of two aldehyde groups and an hydroxyl group. These results indicate a potentially effective application of bio-AuNPs for azo dye decolorization.

Conclusions

In this work, an investigation was conducted to synthesize AuNPs through eco-friendly resource by *M. indicus* CBS 226.29 ET as a newly isolated fungal strain. Characteristics of the biosynthesized AuNPs were ascertained by UV-vis and TEM analysis, and further experiments were made to investigate the effects of certain parameters ($HAuCl_4$ concentrations, biomass concentrations and pH) on AuNPs synthesis to obtain useful data on oriented biosynthesis of AuNPs.

Furthermore, the observations of nanoremediation of various azo dyes as applications of bio-AuNPs indicated good potential application of the biogenetic AuNPs in the decolorization of azo dyes. This work should provide a more insight for using fungi as microbial resource in AuNPs synthesis.

REFERENCES

Bastús NG, Comenge J, Puntes V (2011). Kinetically controlled seeded growth synthesis of citrate-stabilized gold nanoparticles of up to 200 nm: size focusing versus Ostwald ripening. Langmuir. 27(17): 11098-

11105.
Bhumkar DR, Joshi HM, Sastry M, Pokharkar, VB (2007). Chitosan reduced gold nanoparticles as novel carriers for transmucosal delivery of insulin. Pharm. Res. 24 (8): 1415–1426.
Champagne PP, Ramsay JA (2010). Dye decolorization and detoxification by laccase immobilized on porous glass beads. Bioresour. Technol. 101(7): 2230–2235.
Chen XJ, Sun GP, Xu MY (2011). Role of iron in azo reduction by resting cells of *Shewanelladecolorationis* S12. J. Appl. Microbiol. 110(2): 580–586.
Das SK, Das AR, Guha AK (2010). Microbial synthesis of multishaped gold nanostructures. Small 6 (9): 1012–1021.
Dos Santos AB, Cervantes FJ, van Lier JB (2007). Review paper on current technologies for decolourisation of textile wastewaters: perspectives for anaerobic biotechnology. Bioresour. Technol. 98(12): 2369–2385.
Du LW, Xian L, Feng JX (2011). Rapid extra-/intracellular biosynthesis of gold nanoparticles by the fungus *Penicillium* sp. J. Nanopart. Res. 13(3): 921–930.
Fang Y, Xu MY, Wu WM, Chen XJ, Sun GP, Guo J et al. (2015). Characterization of the enhancement of zero valent iron on microbial azo reduction. BMC Microbiol. 15 (1): 85.
Gericke M, Pinches A (2006). Biological synthesis of metal nanoparticles. Hydrometall. 83(1–4): 132–140.
Girard V, Dieryckx C, Job C, Job D (2013). Secretomes: the fungal strike force. Proteomics 13(3–4): 597–608.
Gomi N, Yoshida S, Matsumoto K, Okudomi M, Konno H, Hisabori T, et al. (2011). Degradation of the synthetic dye amaranth by the fungus *Bjerkanderaadusta* Dec 1: inference of the degradation pathway from an analysis of decolorized products. Biodegrad. 22(6): 1239–1245.
Gong JL, Mullins CB (2009). Surface science investigations of oxidative chemistry on gold. Acc. Chem. Res. 42(8): 1063–1073.
Haiss W, Thanh NTK, Aveyard J, Fernig DG (2007). Determination of size and concentration of gold nanoparticles from UV–vis spectra. Anal. Chem. 79(11): 4215–4221.
Kalishwaralal K, Deepak V, Pandian SRK, Gurunathan S (2009). Biological synthesis of gold nanocubes from *Bacillus licheniformis*. Bioresour. Technol. 100(21): 5356–5358.
Kim KW (2008). Vapor fixation of intractable for simple and versatile scanning electron microscopy. J. Phytopathol. 156(2): 125–128.
Kitching M, Ramani M, Marsili E (2015). Fungal biosynthesis of gold nanoparticles: mechanism and scale up. Microb. Biotechnol. 8(6): 904–917.
Kreibig U, Genzel L (1985). Optical absorption of small metallic particles. Surf. Sci. 156(2): 678–700.
Kuang Y, Zhou Y, Chen ZL, Megharaj M, Naidu R (2013). Impact of Fe and Ni/Fe nanoparticles on biodegradation of phenol by the strain *Bacillus fusiformis* (BFN) at various pH values. Bioresour. Technol. 136: 588–594.
Kumari MM, Philip D (2015). Degradation of environment pollutant dyes using phytosynthesized metal nanocatalysts. Spectrochim. Acta. A. Mol. Biomol. Spectrosc. 135: 632–638.
Mishra A, Kumari M, Pandey S, Chaudhry V, Gupta KC, Nautiyal CS (2014). Biocatalytic and antimicrobial activities of gold nanoparticles synthesized by *Trichoderma* sp. Bioresour. Technol. 166: 235–242.
Mishra A, Tripathy SK, Yun SI (2011). Bio-synthesis of gold and silver nanoparticles from *Candida guilliermondii* and their antimicrobial effect against pathogenic bacteria. J. Nanosci. Nanotechnol. 11(1): 243–248.
Morin-sardin S, Nodet P, Coton E, Jany J (2017). Review: Mucor: a janus-faced fungal genus with human health impact and industrial applications. Fungal Bio. Rev. 31(1): 12–32.
Narayanan KB, Sakthivel N (2010). Biological synthesis of metal nanoparticles by microbes. Adv. Colloid Interfaces. Sci. 156(1–2): 1–13.
Pimprikar PS, Joshi SS, Kumar AR, Zinjarde SS, Kulkarni SK 2009. Influence of biomass and gold salt concentration on nanoparticle synthesis by the tropical marine yeast *Yarrowialipolytica* NCIM 3589. Colloids Surf. B. Biointerfaces 74(1): 309–316.
Qu YY, Shi SN, Ma F, Yan B (2010). Decolorization of reactive dark blue KR by the synergism of fungus and bacterium using response surface methodology. Bioresour. Technol. 101(21): 8016–8023.
Shedbalkar U, Singh R, Wadhwani S, Gaidhani S, Chopade BA (2014). Microbial synthesis of gold nanoparticles: current status and future prospects. Adv. Colloid Interface. Sci. 209: 40–48.
Shukla R, Bansal V, Chaudhary M, Basu A, Bhonde RR, Sastry M (2005). Biocompatibility of gold nanoparticles and their endocytotic fate inside the cellular compartment: a microscopic overview. Langmuir 21(23): 10644–10654.
Song JY, Jang HK, Kim BS (2009). Biological synthesis of gold nanoparticles using *Magnolia kobus* and *Diopyros kaki* leaf extracts. Process Biochem. 44(10): 1133–1138.
Sujitha MV, Kannan S (2013). Green synthesis of gold nanoparticles using citrus fruits (*Citrus limon*, *Citrus reticulate* and *Citrus sinensis*) aqueous extract and its characterization. Spectrochim. Acta. A. Mol. Biomol. Spectrosc. 102: 15–23.
Tan L, Ning SX, Zhang XW, Shi SN (2013). Aerobic decolorization and degradation of azo dyes by growing cells of a newly isolated yeast *Candida tropicalis* TL-F1. Bioresour. Technol. 138: 307–313.
Tony BD, Goyal D, Khanna S (2009). Decolorization of textile azo dyes by aerobic bacterial consortium. Int. Biodeterior. Biodegrad. 63(4): 462–469.
Vahabi K, Mansoori GA, Karimi S (2011). Biosynthesis of silver nanoparticles by fungus *Trichoderma reesei* (a route for large-scale production of AgNPs). Insciences J. 1(1): 65–79.
Xu MY, Guo J, Kong XY, Chen XJ, Sun GP (2007). Fe (III)-enhanced azo reduction by *Shewanelladecolorationis* S12. Appl. Microbiol. Biotechnol. 74(6): 1342–1349.
Zhang XL, Yan S, Tyagi RD, Surampalli RY (2011). Synthesis of nanoparticles by microorganisms and their application in enhancing microbiological reaction rates. Chemosphere 82(4): 489–494.

Cite this article as:

Alshehri ANZ (2018). Using a novel *Mucorindicus* CBS 226.29 ET for Biosynthesis of gold nanoparticles and applying them in nanoremediation of azo dyes. Acad. J. Biotechnol. 6(1): 001-011.

Submit your manuscript at
http://www.academiapublishing.org/ajb